

ATLab Documentation

Turbulence and Boundary Layers Group | University of Hamburg

February 16, 2026

Contents

Preface	v
I User Guide	1
1 Governing equations	3
1.1 Evolution equations	3
1.1.1 Boussinesq	3
1.1.2 Anelastic	4
1.1.3 Compressible	4
1.2 Thermodynamics	5
1.2.1 Compressible	5
1.2.2 Anelastic	5
1.2.3 Mixtures	6
2 Post-Processing Tools	9
2.1 Averages	9
2.2 Summary of budget equations for second-order moments	9
2.2.1 Reynolds Stresses	11
2.2.2 Scalar Fluxes	11
2.2.3 Scalar Variance	12
II Technical Guide	13
3 Numerical Algorithms	15
3.1 Spatial operators	15
3.1.1 Derivatives	15
3.1.2 Fourier transform	15
3.1.3 Poisson equation	16
3.1.4 Helmholtz equation	16
3.2 Time marching schemes	16
3.2.1 Explicit schemes	16
3.2.2 Implicit schemes	16
4 Memory management	17
5 Profiling	19

Preface

ATLab—an acronym for Atmospheric Turbulence Laboratory—is a set of tools to solve and analyze various forms of the governing equations commonly used to study atmospheric turbulence. The emphasis is on efficiency and controlled accuracy, and less on having a user-friendly, general purpose code.

The accuracy can be controlled in different ways: comparing with analytical solutions, including linear stability analysis; grid convergence studies; balance of transport equations, like integral turbulent kinetic energy or local values at specific relevant locations (e.g., at the wall). Resolution can be measured by the ratio between the grid spacing Δx and the relevant small scales, like the Kolmogorov scale η or the thickness of the diffusion sub-layers next to the wall. For the compact schemes used here, typical values are $\Delta x/\eta \simeq 1 - 2$; larger values can lead to numerical instability because of the aliasing generated by the non-linear terms. Note that these schemes are non-monotone, but typical out-of-bounds deviations of conserved scalars are below $10^{-6} - 10^{-8}$ relative to the mean variations, and this error is therefore negligibly small compared to the typical error associated with the statistical convergence, of the order of 1 – 5%. The statistical convergence can be estimated by varying the sample size of the data set, e.g. varying the domain size along the statistically homogeneous directions.

The efficiency can be measured in different ways but, ultimate, it should be related with the computational time needed to understand a particular problem with a given accuracy, and so the importance of the controlled accuracy.

Last, the main documentation is the code itself and the examples. This document is only a short introduction to the equations and the tools. The code is continuously under development, so this document is continuously incomplete.

Part I

User Guide

Chapter 1

Governing equations

The code is built to solve the sets of equations described in this section as efficiently as possible. These sets of equations aim to be general enough to cover several problems. As a consequence, one needs to map particular problems to one of these generic cases, and identify the appropriate values of the parameters and defining functions (for instance, Re or b^e). Certain knowledge of the equations is therefore advantageous.

1.1 Evolution equations

1.1.1 Boussinesq

Dynamics and thermodynamics are at most coupled by the buoyancy field, and thermodynamics is not necessary (but can still be used). We consider the momentum equation and the evolution equations for an arbitrary number of scalar fields in the following form:

$$\partial_t v_i = -v_k \partial_k v_i + \partial_k (\text{Re}^{-1} \nu \partial_k v_i) - \partial_i p' + \text{Fr}^{-1} g_i b + \text{Ro}^{-1} \epsilon_{ijk} f_k v_k , \quad i = 1, 2, 3 \quad (1.1a)$$

$$\partial_t s_i = -v_k \partial_k s_i + \partial_k [(\text{ReSc}_i)^{-1} \nu \partial_k s_i - \partial_k (\mathbf{j}_i)_k] + \omega_i , \quad i = 1, \dots, n \quad (1.1b)$$

The dynamic variables in these equations are nondimensionalized by ρ_0 , U_0 and L_0 . The parameters Re, Sc, Fr and Ro need to be provided.

- The scalar field ν represents the kinematic viscosity. In the simplest case, it is equal to 1.
- The scalar field b represents the buoyancy, if any. The vector (g_i) gives the direction of the buoyancy force and it is constant.
- The vector fields \mathbf{j}_i represent flux terms, if any.
- The scalar fields ω_i represent source terms, if any.

These fields are defined in terms of the scalars s_k by functions $\nu^e(s_k)$, $b^e(s_k)$, $\mathbf{j}_i^e(s_k)$ and $\omega_i^e(s_k)$, to be given.

- The vector (f_i) gives the direction of the angular velocity of the frame of reference, if any. It is assumed constant.

Mass conservation,

$$\partial_k v_k = 0 , \quad (1.2)$$

is imposed in terms of the pressure-Poisson equation

$$\nabla^2 p' = \partial_k(\dots) \quad (1.3)$$

with the boundary conditions that result from particularizing the momentum equation at the top and bottom boundaries. Details can be found in Mellado and Ansorge [2012].

Dimensional Formulation

A dimensional formulation can be considered by substituting the parameters **Reynolds**, **Froude** and **Rossby** the input file (by default, `tlab.ini`) with **Viscosity**, **Gravity** and **Coriolis**. The boundary and initial conditions defined in the input file should then be given in dimensional form.

1.1.2 Anelastic

Dynamics and thermodynamics are coupled by the density. The momentum equation is formulated in terms of the dynamic pressure and the density:

$$\partial_t v_i = -v_k \partial_k v_i + \rho_{\text{bg}}^{-1} \partial_k (\text{Re}^{-1} \mu \partial_k v_i) - \rho_{\text{bg}}^{-1} \partial_k p' + \text{Fr}^{-1} g_i (1 - \rho / \rho_{\text{bg}}) + \text{Ro}^{-1} \epsilon_{ijk} f_k v_k . \quad (1.4)$$

The evolution equations for the scalars read:

$$\partial_t s_i = -v_k \partial_k s_i + \rho_{\text{bg}}^{-1} \partial_k [(\text{Re} \text{Sc}_i)^{-1} \mu \partial_k s_i - \partial_k (\mathbf{j}_i)_k] + \omega_i , \quad i = 1, \dots, n \quad (1.5)$$

Symbols are as explained in the Boussinesq case. The scalar field μ represents the dynamic viscosity. In the simplest case, it is equal to 1.

Mass conservation,

$$\partial_k (\rho_{\text{bg}} v_k) = 0 , \quad (1.6)$$

is imposed in terms of the pressure-Poisson equation

$$\nabla^2 p' = \partial_k (\rho_{\text{bg}} \dots) \quad (1.7)$$

with the boundary conditions that result from particularizing the momentum equation at the top and bottom boundaries

1.1.3 Compressible

Dynamics and thermodynamics are fully coupled. The pressure in the momentum equation is the thermodynamic pressure. Mass conservation is expressed in terms of the evolution equation

$$\partial_t \rho = -\partial_k (\rho v_k) \quad (1.8)$$

instead of a solenoidal constraint.

The variables in these equations are normalized by the reference scales L_0 , U_0 , ρ_0 and T_0 , which represent a length, a velocity, a density, and a temperature, respectively. The pressure is normalized by $\rho_0 U_0^2$.

TBD

1.2 Thermodynamics

We consider n_c components (or species) with mass fractions ζ_i .

1.2.1 Compressible

The thermal equation of state is implemented as

$$p = \rho RT . \quad (1.9)$$

The scalar field

$$R = \sum_1^{n_c} R_i \zeta_i \quad (1.10)$$

is the specific gas constant of the mixture.

The caloric equation of state is implemented as

$$h = \sum_1^{n_c} h_i \zeta_i , \quad h_i = \Delta h_i^0 + \int_{T_0}^T c_{pi}(T) dT . \quad (1.11)$$

Each species has a specific heat capacity c_{pi} and a specific gas constant $R_i = \mathcal{R}/W_i$, where \mathcal{R} is the universal gas constant and W_i the molar mass of the species. They are nondimensionalized by the reference values c_{p0} and $R_0 = \mathcal{R}/W_0$, respectively, which are the values of one of the species.

The thermodynamic variables are nondimensionalized as in evolution equations, i.e., the reference scales L_0 , U_0 , ρ_0 and T_0 , which represent a length, a velocity, a density, and a temperature, respectively. The pressure is normalized by $\rho_0 U_0^2$. Thermal energy variables are normalized with $c_{p0} T_0$, where c_{p0} is a reference specific heat capacity at constant pressure.

TBD

Dimensional Formulation

In this case of a multi-species, a dimensional formulation can be considered by setting the input parameter `nondimensional` equal to `.false.` in the block `[Thermodynamics]` of the input file (by default, `tlab.ini`).

1.2.2 Anelastic

The thermal equation of state is implemented as

$$p_{bg} = \rho RT . \quad (1.12)$$

The thermodynamic variables are nondimensionalized by ρ_0 , T_0 and R_0 , such that $p_0 = \rho_0 R_0 T_0$. The default reference values are $p_0 = 10^5$ Pa and $T_0 = 298$ K. Thermal energy variables are normalized with $c_{p0} T_0$, where c_{p0} is a reference specific heat capacity at constant pressure.

The caloric equation of state is formulated in terms of the static energy

$$h = \sum_1^{n_c} h_i \zeta_i + \frac{\gamma_0 - 1}{\gamma_0} H^{-1}(x_3 - x_{3,0}) . \quad (1.13)$$

The scalar field c is the specific heat capacity, a function of the scalars s_i . The parameter

$$H = \frac{R_0 T_0}{g L_0} \quad (1.14)$$

is a nondimensional scale height, or the inverse of a nondimensional gravity, to be provided. The parameter

$$R_0/c_{p0} = (\gamma_0 - 1)/\gamma_0 , \quad (1.15)$$

a conversion factor between gas constants and heat capacities (thermal equation of state and caloric equation of state). We refer to it in the code as **GRATIO**.

The background profiles $\{\rho_{\text{bg}}, p_{\text{bg}}, T_{\text{bg}}, \zeta_{i,\text{ref}}\}$ correspond to a state of thermodynamic and hydrostatic equilibrium. The code solves the system of equations

$$\partial_3 p_{\text{bg}} = -H^{-1} g_3 \rho_{\text{bg}} , \quad p_{\text{bg}}|_{x_3=x_{3,0}} = p_{\text{bg},0} , \quad (1.16a)$$

$$\rho_{\text{bg}} = \rho_{\text{bg}} R_{\text{bg}} T_{\text{bg}} . \quad (1.16b)$$

g is defined opposite to the gravitational acceleration (the problem is formulated in terms of the buoyancy). The two equations above relate 4 thermodynamic variables and we need two additional constraints. Typically, we impose the background profile of static energy (enthalpy plus potential energy) and the composition. If there is only one species, then $R_{\text{bg}} = 1$ and we only need one additional constraint.

Currently implemented only for air-water mixtures. In this case, the first scalar is the energy variable and the remaining scalars are the composition (e.g., total water specific humidity and liquid water specific humidity).

Dimensional Formulation

A dimensional formulation can be considered by setting the parameter **nondimensional** equal to `.false.`, which sets **GRATIO** equal to 1

1.2.3 Mixtures

We consider n_c components (or species) with mass fractions ζ_i . These need not be equal to the prognostic scalar variables s_k , and the relationship between them $\zeta_i = \zeta_i^e(s_k)$ needs to be given.

In the generic case, we choose

$$\zeta_i = s_i , \quad i = 1, \dots, n_c - 1 , \quad (1.17)$$

and the last component has a mass fraction

$$\zeta_{n_c} = 1 - \sum_1^{n_c-1} \zeta_i . \quad (1.18)$$

The gas constant can then be written as

$$R = \sum_1^{n_c} \zeta_i R_i = \sum_1^{n_c-1} (R_i - R_N) , \quad (1.19)$$

and similarly for other thermodynamic variables.

Particular cases different from this one occur for instance when we consider chemical equilibrium or phase equilibrium, or when different combinations of mass fractions might be preferable to better represent conservation properties.

Air-water mixtures in anelastic formulations

We consider the total water specific humidity as prognostic variable. If necessary, we also consider the liquid water specific humidity, which can be diagnostic in the case of phase equilibrium, or prognostic otherwise.

Chapter 2

Post-Processing Tools

2.1 Averages

See file `dns/tools/postprocessing/averages`.

Allows for conditional analysis.

2.2 Summary of budget equations for second-order moments

Let f and g be fluid properties per unit mass. We use the Reynolds decomposition

$$f = \bar{f} + f' , \quad (2.1)$$

and the Favre decomposition

$$f = \tilde{f} + f'' , \quad (2.2)$$

where

$$\tilde{f} = \overline{\rho f} / \bar{\rho} . \quad (2.3)$$

Favre decomposition proves convenient in variable-density flows. The overbar indicates ensemble average, which is approximated by spatial average, or temporal average, or both, depending on the configuration. We will refer to it as Reynolds average, and use the term Favre average to refer to the density-weighted averages (property per unit volume). Note that $\tilde{f}'' = 0$ and $\bar{f}' = 0$, but

$$\overline{f''} = \bar{f} - \tilde{f} , \quad (2.4)$$

which is zero in constant-density flows, when \bar{f} and \tilde{f} coincide. The covariances satisfy

$$\overline{f'g'} = \bar{f}g' = \bar{f}'\bar{g} = \overline{f'g''} = \overline{f''g'} = \bar{f}\bar{g} - \bar{f}\bar{g} , \quad (2.5)$$

$$\widetilde{f''g''} = \widetilde{f}\widetilde{g''} = \widetilde{f''}\widetilde{g} = \widetilde{f'}\widetilde{g''} = \widetilde{f''}\widetilde{g'} = \widetilde{f}\widetilde{g} - \widetilde{f}\widetilde{g} , \quad (2.6)$$

$$\overline{fg} - \overline{f}\overline{g} = \overline{f''g'} - \overline{f}\overline{g''} . \quad (2.7)$$

We consider evolution equations of the following form:

$$\partial_t (\rho f) + \nabla \cdot (\rho f \mathbf{v}) = -\nabla \cdot \mathbf{F} + \rho S_f , \quad (2.8a)$$

$$\partial_t (\rho g) + \nabla \cdot (\rho g \mathbf{v}) = -\nabla \cdot \mathbf{G} + \rho S_g . \quad (2.8b)$$

Multiplying the first equation by g and the second by f and adding them, one finds the evolution equation for the product $\rho f g$:

$$\begin{aligned}\partial_t(\rho f g) + \nabla \cdot (\rho f g \mathbf{v}) &= -g \nabla \cdot \mathbf{F} - f \nabla \cdot \mathbf{G} \\ &\quad + \rho g S_f + \rho f S_g ,\end{aligned}\tag{2.9}$$

having used the equation of conservation of mass

$$\partial_t \rho + \nabla \cdot (\rho \mathbf{v}) = 0\tag{2.10}$$

in the left hand side.

The evolution equation for the mean properties can be written as

$$\partial_t(\bar{\rho} \tilde{f}) + \nabla \cdot (\bar{\rho} \tilde{f} \tilde{\mathbf{v}}) = -\nabla \cdot (\bar{\mathbf{F}} + \bar{\rho} \tilde{f}'' \tilde{\mathbf{v}}'') + \bar{\rho} \tilde{S}_f ,\tag{2.11a}$$

$$\partial_t(\bar{\rho} \tilde{g}) + \nabla \cdot (\bar{\rho} \tilde{g} \tilde{\mathbf{v}}) = -\nabla \cdot (\bar{\mathbf{G}} + \bar{\rho} \tilde{g}'' \tilde{\mathbf{v}}'') + \bar{\rho} \tilde{S}_g .\tag{2.11b}$$

Multiplying the first equation by \tilde{g} and the second by \tilde{f} and adding them, one finds the evolution equation for the product $\bar{\rho} \tilde{f} \tilde{g}$:

$$\begin{aligned}\partial_t(\bar{\rho} \tilde{f} \tilde{g}) + \nabla \cdot (\bar{\rho} \tilde{f} \tilde{g} \tilde{\mathbf{v}}) &= -\tilde{g} \nabla \cdot \bar{\mathbf{F}} - \tilde{f} \nabla \cdot \bar{\mathbf{G}} \\ &\quad - \nabla \cdot (\bar{\rho} \tilde{f}'' \tilde{\mathbf{v}}'' \tilde{g} + \bar{\rho} \tilde{g}'' \tilde{\mathbf{v}}'' \tilde{f}) \\ &\quad + \bar{\rho} \tilde{\mathbf{v}}'' \tilde{f}'' \cdot \nabla \tilde{g} + \bar{\rho} \tilde{\mathbf{v}}'' \tilde{g}'' \cdot \nabla \tilde{f} \\ &\quad + \tilde{g} \bar{S}_f + \tilde{f} \bar{S}_g ,\end{aligned}\tag{2.12}$$

having used the equation of conservation of mass

$$\partial_t \bar{\rho} + \nabla \cdot (\bar{\rho} \tilde{\mathbf{v}}) = 0\tag{2.13}$$

in the left hand side.

Averaging Eq. (2.9) and subtracting Eq. (2.12) from it, one finds

$$\begin{aligned}\partial_t(\bar{\rho} \tilde{f}'' \tilde{g}'') + \nabla \cdot (\bar{\rho} \tilde{f}'' \tilde{g}'' \tilde{\mathbf{v}}) &= -\nabla \cdot (\bar{\rho} \tilde{\mathbf{v}}'' \tilde{f}'' \tilde{g}'' + \bar{\mathbf{F}}' \tilde{g}'' + \bar{\mathbf{G}}' \tilde{f}'') \\ &\quad + \bar{\mathbf{F}}' \cdot \nabla \tilde{g}'' + \bar{\mathbf{G}}' \cdot \nabla \tilde{f}'' \\ &\quad - \bar{\rho} \tilde{\mathbf{v}}'' \tilde{f}'' \cdot \nabla \tilde{g} - \bar{\rho} \tilde{\mathbf{v}}'' \tilde{g}'' \cdot \nabla \tilde{f} \\ &\quad + \bar{\rho} \tilde{S}_f'' \tilde{g}'' + \bar{\rho} \tilde{S}_g'' \tilde{f}'' \\ &\quad - \bar{g}'' \nabla \cdot \bar{\mathbf{F}} - \bar{f}'' \nabla \cdot \bar{\mathbf{G}} ,\end{aligned}\tag{2.14}$$

having used the relationship

$$\overline{\rho f g \mathbf{v}} = \bar{\rho} \tilde{f} \tilde{g} \tilde{\mathbf{v}} + \bar{\rho} \tilde{\mathbf{v}}'' \tilde{f}'' \tilde{g}'' + \tilde{f}'' \tilde{g}'' \tilde{\mathbf{v}} + \tilde{f}'' \tilde{\mathbf{v}}'' \tilde{g} + \tilde{g}'' \tilde{\mathbf{v}}'' \tilde{f} ,\tag{2.15}$$

together with

$$\begin{aligned}\overline{g \nabla \cdot \mathbf{F} - \tilde{g} \nabla \cdot \bar{\mathbf{F}}} &= \overline{g'' \nabla \cdot \mathbf{F}'} + \overline{g'' \nabla \cdot \bar{\mathbf{F}}} \\ &= \nabla \cdot (\bar{\mathbf{F}}' g'') - \bar{\mathbf{F}}' \cdot \nabla g'' + \bar{g}'' \nabla \cdot \bar{\mathbf{F}}\end{aligned}\tag{2.16}$$

and similarly for the other second-order term $f \nabla \cdot \mathbf{G}$.

2.2.1 Reynolds Stresses

Consider the momentum equations:

$$f = u_i , \quad F_k = p \delta_{ik} - \tau_{ik} , \quad S_f = b g_i - \epsilon_{imk} f_m u_k , \quad (2.17)$$

$$g = u_j , \quad G_k = p \delta_{jk} - \tau_{jk} , \quad S_g = b g_j - \epsilon_{jmk} f_m u_k . \quad (2.18)$$

Substituting into Eq. (2.14), we find

$$\partial_t R_{ij} = C_{ij} + P_{ij} - E_{ij} + \bar{\rho}^{-1} (\Pi_{ij} - \partial_k T_{ijk} + M_{ij}) + B_{ij} - F_{ij} \quad (2.19)$$

where

$$\begin{aligned} R_{ij} &= \widetilde{u''_i u''_j} && \text{(Reynolds-stress component)} \\ C_{ij} &= -\widetilde{u}_k \partial_k R_{ij} && \text{(mean advection)} \\ P_{ij} &= -R_{ik} \partial_k \widetilde{u}_j - R_{jk} \partial_k \widetilde{u}_i && \text{(mean-gradient (shear) production)} \\ E_{ij} &= \bar{\rho}^{-1} (\overline{\tau'_{jk}} \partial_k u''_i + \overline{\tau'_{ik}} \partial_k u''_j) && \text{(viscous dissipation)} \\ T_{ijk} &= \overline{\rho u''_i u''_j u''_k} + \overline{p' u'_i} \delta_{jk} + \overline{p' u'_j} \delta_{ik} - (\overline{\tau'_{jk}} u''_i + \overline{\tau'_{ik}} u''_j) && \text{(turbulent transport)} \\ \Pi_{ij} &= \overline{p'} (\partial_j u''_i + \partial_i u''_j) && \text{(pressure strain)} \\ M_{ij} &= \overline{u''_i} (\partial_k \bar{\tau}_{jk} - \partial_j \bar{p}) + \overline{u''_j} (\partial_k \bar{\tau}_{ik} - \partial_i \bar{p}) && \text{(mean flux)} \\ B_{ij} &= \overline{b'' u''_j} g_i + \overline{b'' u''_i} g_j && \text{(buoyancy production-destruction)} \\ F_{ij} &= \epsilon_{imk} f_m R_{jk} + \epsilon_{jmk} f_m R_{ik} && \text{(Coriolis redistribution)} \end{aligned}$$

Depending on symmetries, several terms can be zero (within statistical convergence). Note that if $b \equiv 1$, then $B_{ij} = 0$. The mean flux term is sometimes written as $M_{ij} = D_{ij} - G_{ij}$, the first term grouping the mean viscous stress contributions and the last term the mean pressure contributions. In cases of constant density, then $\overline{u''_j} = 0$ and $M_{ij} = D_{ij} = G_{ij} = 0$.

Contracting indices, the budget equation for the turbulent kinetic energy $K = R_{ii}/2$ reads

$$\partial_t K = C + P + B - E + \bar{\rho}^{-1} (\Pi - \partial_k T_k + M) . \quad (2.20)$$

Note that $F_{ii} = 0$. If the flow is solenoidal, then $\Pi = 0$.

2.2.2 Scalar Fluxes

Consider the momentum and scalar equations:

$$f = u_i , \quad F_k = p \delta_{ik} - \tau_{ik} , \quad S_f = b g_i - \epsilon_{imk} f_m u_k , \quad (2.21)$$

$$g = \zeta , \quad G_k = -q_k , \quad S_g = w . \quad (2.22)$$

Substituting into Eq. (2.14), we find

$$\partial_t R_{i\zeta} = C_{i\zeta} + P_{i\zeta} - E_{i\zeta} + \bar{\rho}^{-1} (\Pi_{i\zeta} - \partial_k T_{i\zeta k} + M_{i\zeta}) + B_{i\zeta} - F_{i\zeta} + Q_{i\zeta} \quad (2.23)$$

where

$$\begin{aligned}
 R_{i\zeta} &= \widetilde{u''_i \zeta''} && \text{(scalar-flux component)} \\
 C_{i\zeta} &= -\tilde{u}_k \partial_k R_{i\zeta} && \text{(mean advection)} \\
 P_{i\zeta} &= -R_{ik} \partial_k \tilde{\zeta} - R_{\zeta k} \partial_k \tilde{u}_i && \text{(mean-gradient and tilting production)} \\
 E_{i\zeta} &= \bar{\rho}^{-1} (\bar{q}'_k \partial_k u''_i + \bar{\tau}'_{ik} \partial_k \zeta'') && \text{(molecular destruction)} \\
 \Pi_{i\zeta} &= \overline{p' \partial_i \zeta''} && \text{(pressure-flux interaction)} \\
 T_{i\zeta k} &= \overline{\rho \zeta'' u''_k u''_i} + \overline{p' s''} \delta_{ik} - \overline{\tau'_{ik} s''} - \overline{q'_k u''_i} && \text{(turbulent transport)} \\
 M_{i\zeta} &= \overline{u''_i \partial_k \bar{q}_k} + \overline{\zeta''} (\partial_k \bar{\tau}_{ik} - \partial_i \bar{p}) && \text{(mean flux)} \\
 B_{i\zeta} &= \widetilde{b'' \zeta'' g_i} && \text{(buoyancy iteration)} \\
 F_{i\zeta} &= \epsilon_{imk} f_m R_{k\zeta} && \text{(Coriolis interation)} \\
 Q_{i\zeta} &= \widetilde{w'' u''_i} && \text{(source)}
 \end{aligned}$$

The mean flux term is sometimes written as $M_{i\zeta} = D_{i\zeta} - G_{i\zeta}$, the first term grouping the mean molecular flux contributions and the last term the mean pressure contributions.

2.2.3 Scalar Variance

Consider the scalar equation twice:

$$f = \zeta , \quad F_k = -q_k , \quad S_f = w , \quad (2.24)$$

$$g = \zeta , \quad G_k = -q_k , \quad S_g = w . \quad (2.25)$$

Substituting into Eq. (2.14), we find

$$\partial_t R_{\zeta\zeta} = C_{\zeta\zeta} + P_{\zeta\zeta} - E_{\zeta\zeta} + \bar{\rho}^{-1} (-\partial_k T_{\zeta\zeta k} + M_{\zeta\zeta}) + Q_{\zeta\zeta} \quad (2.26)$$

where

$$\begin{aligned}
 R_{\zeta\zeta} &= \widetilde{\zeta'' \zeta''} && \text{(scalar variance)} \\
 C_{\zeta\zeta} &= -\tilde{u}_k \partial_k R_{\zeta\zeta} && \text{(mean advection)} \\
 P_{\zeta\zeta} &= -2R_{k\zeta} \partial_k \tilde{\zeta} && \text{(mean-gradient production)} \\
 E_{\zeta\zeta} &= 2\bar{\rho}^{-1} \bar{q}'_k \partial_k \zeta'' && \text{(molecular destruction)} \\
 T_{\zeta\zeta k} &= \overline{\rho \zeta''^2 u''_k} - 2\overline{q'_k \zeta''} && \text{(turbulent transport)} \\
 M_{\zeta\zeta} &= 2\overline{\zeta''} \partial_k \bar{q}_k && \text{(mean flux)} \\
 Q_{\zeta\zeta} &= 2\widetilde{w'' \zeta''} && \text{(source)}
 \end{aligned}$$

Part II

Technical Guide

Chapter 3

Numerical Algorithms

The system of equations is written as

$$\partial_t \mathbf{q} = \mathbf{F}_q(\mathbf{q}, \mathbf{s}, t), \quad (3.1a)$$

$$\partial_t \mathbf{s} = \mathbf{F}_s(\mathbf{q}, \mathbf{s}, t). \quad (3.1b)$$

where \mathbf{q} and \mathbf{s} are the vector vectors of flow and scalar prognostic variables. For the incompressible formulations, we have

$$\mathbf{q} = (u_1, u_2, u_3)^T, \quad (3.2a)$$

$$\mathbf{s} = (s_1, s_2, \dots)^T. \quad (3.2b)$$

The code uses the method of lines, so that the algorithm is a combination of different spatial operators that calculate the right-hand side of the equations and a time marching scheme.

3.1 Spatial operators

Spatial operators are based on finite difference methods (FDM). There are two levels of routines. The low-level libraries contain the basic algorithms and are explained in this section. It consists of the FDM kernel library `finitedifferences` and three-dimensional operators library `operators`. The high-level library `mappings` is composed of routines that are just a combination of the low-level routines.

3.1.1 Derivatives

See file `operators/opr_partial`.

Spatial derivatives are calculated using fourth- or sixth-order compact Padé schemes as described by Lele [1992] and Lamballais et al. [2011] for uniform grids and extended by Shukla and Zhong [2005] for non-uniform grids. The kernels of the specific algorithms are in the library `finitedifferences`.

3.1.2 Fourier transform

See file `operators/opr_fourier`.

It is based on the FFTW library [Frigo and Johnson, 2005].

3.1.3 Poisson equation

See file `operators/opr_elliptic.`

Given the scalar field s , obtain the scalar field f such that

$$\nabla^2 f = s , \quad (3.3)$$

complemented with appropriate boundary conditions. The current version only handles cases with periodic boundary conditions along Ox and Oy . It performs a Fourier decomposition along these two directions, to obtain the a set of finite difference equations along Oz of the form

$$\delta_x \delta_x \mathbf{f}|_j - (\lambda_1/h)^2 \mathbf{f}|_j = \mathbf{s}|_j , \quad j = 2, \dots, n-1 , \quad (3.4)$$

$\lambda_1 \in \mathbb{R}$, where boundary conditions need to be provided at $j = 1$ and $j = n$. The algorithm is described in Mellado and Ansorge [2012]. We can also consider the case in which the second-order derivative is implemented in terms of the δ_{xx} FDM operator, not only the $\delta_x \delta_x$ FDM operator. These routines are in the source file `operators/opr_odes.`

3.1.4 Helmholtz equation

See file `operators/opr_elliptic.`

Given the scalar field s , obtain the scalar field f such that

$$\nabla^2 f + \alpha f = s , \quad (3.5)$$

complemented with appropriate boundary conditions. The current version only handles cases with periodic boundary conditions along Ox and Oy . The algorithm is similar to that used for the Poisson equation. It performs a Fourier decomposition along these two directions, to obtain the a set of finite difference equations along Oz of the form

$$\delta_x \delta_x \mathbf{f}|_j - (\lambda_2/h^2 - \alpha) \mathbf{f}|_j = \mathbf{s}|_j , \quad j = 2, \dots, n-1 , \quad (3.6)$$

$\lambda_2 \in \mathbb{R}$, where boundary conditions need to be provided at $j = 1$ and $j = n$.

3.2 Time marching schemes

See file `tools/simulation/timemarching.`

The time advancement is based on Runge-Kutta methods (RKM).

3.2.1 Explicit schemes

We can use three- or five-stages, low-storage RKM that gives third- or fourth-order accurate temporal integration, respectively [Williamson, 1980, Carpenter and Kennedy, 1994]. The stability properties for the biased finite difference schemes are considered in Carpenter et al. [1993]. The incompressible formulation follows Williamson [1980].

3.2.2 Implicit schemes

An implicit treatment of the diffusive terms in the incompressible case follows Spalart et al. [1991]. TBD.

Chapter 4

Memory management

See file `base/tlab_memory`.

Main arrays are allocated during initialization. Intermediate variables are to be stored in `tmp` and not in scratch arrays. Scratch arrays can always be used in low level procedures (e.g., `finitendifferences`), and it is better not to use them in high level procedures (e.g., `operators`).

array	size	content
<code>x</code>	number of points in Ox	x -coordinate information
<code>y</code>	number of points in Oy	y -coordinate information
<code>z</code>	number of points in Oz	z -coordinate information
<code>g</code>	number of points in each direction \times number of arrays for numerics	finite differences information
<code>q</code>	number of points \times number of flow fields	flow variables
<code>s</code>	number of points \times number of scalar fields	scalar variables
<code>txc</code>	extended number of points \times number of temporary fields	temporary variables
<code>wrk3d</code>	extended number of points	scratch
<code>wrk2d</code>	maximum number of points in 2D planes \times number of scratch planes	scratch
<code>wrk1d</code>	maximum number of points in 1D lines \times number of scratch lines	scratch

Table 4.1: Main arrays and their sizes in terms of the number of points. The first 4 are derived types.

Pointers are also defined during initialization to access these memory spaces with arrays of different shape and even different type, more specifically, complex type needed in Fourier decomposition. See corresponding procedures in `base/tlab_memory`.

Chapter 5

Profiling

Profiling data obtained from gfortran -pg and processed with gprof, running the command `gprof path/to/your/executable | gprof2dot --color-nodes-by-selftime | dot -Tpdf -o output.pdf`.

The diagrams been constructed with `gprof2dot.py`¹.

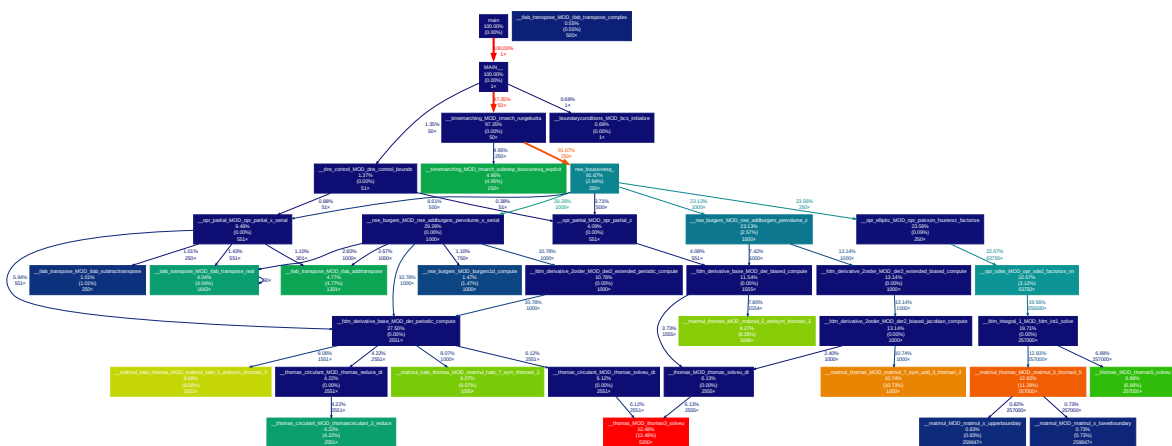


Figure 5.1: Profiling diagram of `examples/Case08` running 50 iterations in serial mode.

¹<https://github.com/jrfonseca/gprof2dot>

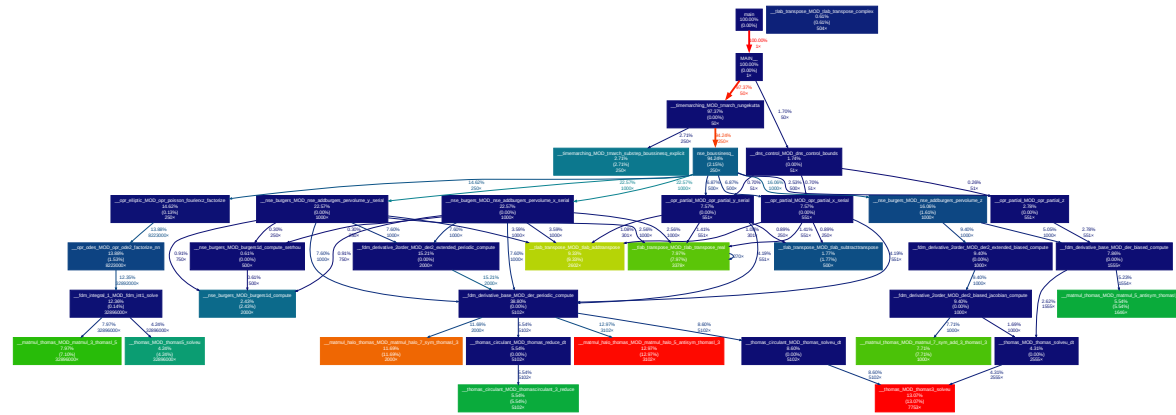


Figure 5.2: Profiling diagram of examples/Case08-3d running 50 iterations in serial mode.

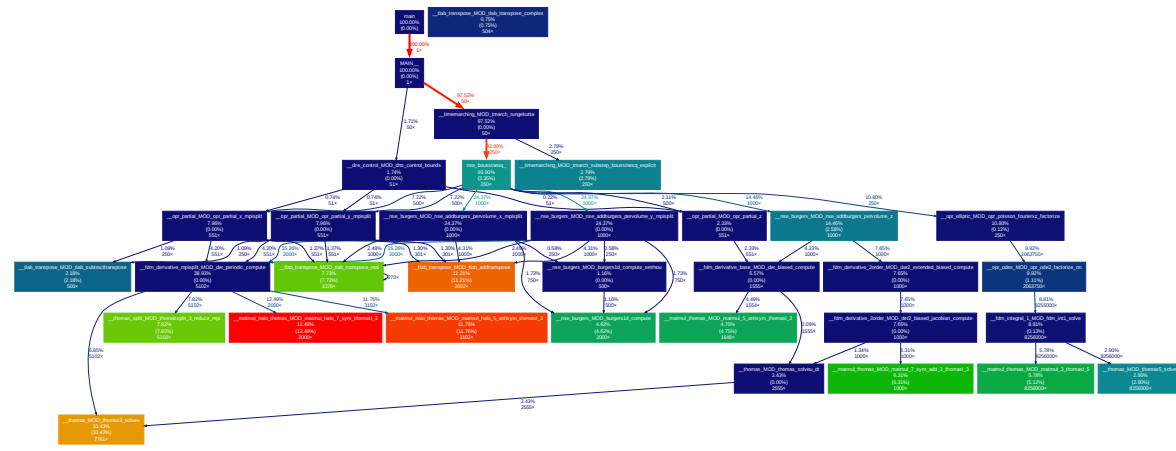


Figure 5.3: Profiling diagram of examples/Case08-3d running 50 iterations in parallel mode with 4 processors.

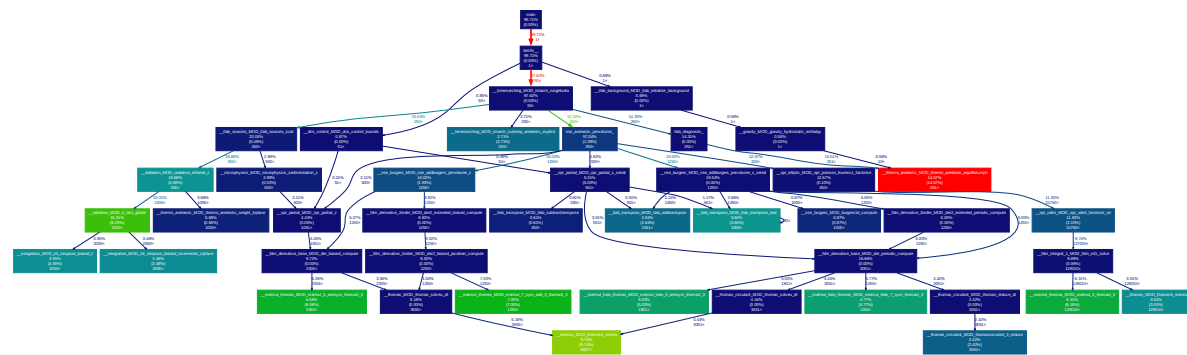


Figure 5.4: Profiling diagram of `examples/Case65` running 50 iterations in serial mode.

Bibliography

- Mark H Carpenter and Christopher A Kennedy. Fourth-order 2n-storage runge-kutta schemes. Technical Report TM-109112, NASA Langley Research Center, 1994.
- Mark H Carpenter, David Gottlieb, and Saul Abarbanel. The stability of numerical boundary treatments for compact high-order finite-difference schemes. *Journal of Computational Physics*, 108(2):272–295, 1993.
- Matteo Frigo and Steven G Johnson. The design and implementation of fftw3. *Proceedings of the IEEE*, 93(2): 216–231, 2005.
- Eric Lamballais, Véronique Fortuné, and Sylvain Laizet. Straightforward high-order numerical dissipation via the viscous term for direct and large eddy simulation. *Journal of Computational Physics*, 230(9):3270–3275, 2011.
- Sanjiva K Lele. Compact finite difference schemes with spectral-like resolution. *Journal of computational physics*, 103(1):16–42, 1992.
- Juan Pedro Mellado and Cedrick Ansorge. Factorization of the fourier transform of the pressure-poisson equation using finite differences in colocated grids. *ZAMM-Journal of Applied Mathematics and Mechanics/Zeitschrift für Angewandte Mathematik und Mechanik*, 92(5):380–392, 2012.
- Ratnesh K Shukla and Xiaolin Zhong. Derivation of high-order compact finite difference schemes for non-uniform grid using polynomial interpolation. *Journal of Computational Physics*, 204(2):404–429, 2005.
- Philippe R Spalart, Robert D Moser, and Michael M Rogers. Spectral methods for the navier-stokes equations with one infinite and two periodic directions. *Journal of Computational Physics*, 96(2):297–324, 1991.
- John H Williamson. Low-storage runge-kutta schemes. *Journal of computational physics*, 35(1):48–56, 1980.